

## ELECTRON AND ION CONTRIBUTIONS TO THE STARK BROADENING IN THE He I SPECTRUM

V. MILOSAVLJEVIĆ

*Faculty of Physics, University of Belgrade, P.O.B. 368, Belgrade, Serbia  
E-mail: vladimir@ff.bg.ac.yu*

**Abstract.** Stark broadening parameters of seven (388.86, 447.15, 471.32, 501.56, 587.56, 667.82 and 706.52 nm) He I spectral line profiles have been measured at electron densities and electron temperatures between  $0.3 \times 10^{22}$  and  $8.2 \times 10^{22}$  m<sup>-3</sup> and 8 000 and 33 000 K, respectively. He I spectral line profiles have been measured in plasmas created in five various discharge conditions using a linear, low-pressure, pulsed arc as an optically thin plasma source operated in a helium–nitrogen–oxygen gas mixture. The influence of electrons and ions to above mention He I spectral line shapes has been studied in this work. On the basis of the observed asymmetry of the line profiles, their ion broadening parameters ( $A$ ) caused by influence of the ion microfield on the line broadening mechanism and also by the influence of the ion dynamic effect ( $D$ ) on the line shape, the  $A$  and  $D$  parameters have been obtained. They represent the first data obtained experimentally by the use of the line profile deconvolution procedure. Stronger influence of the ion contribution to these He I line shapes has been found than the semiclassical theoretical approximation provides. This can be important for plasma modeling or diagnostics.

Also, on the basis of the precisely recorded He I line profiles the basic plasma parameters i.e. electron temperature ( $T$ ) and electron density ( $N$ ) have been obtained using the new line deconvolution procedure. The plasma parameters have been also measured using independent experimental diagnostical techniques. Excellent agreement was found among the two sets of the obtained parameters. This enables the deconvolution procedure to be recommended for plasma diagnostical purposes, especially in astrophysics where direct measurements of the plasma parameters ( $T$  and  $N$ ) are not possible.

### 1. INTRODUCTION

Spectral line shapes represent important sources of information about the physical conditions in the place of birth of the radiation, especially since the launching of the Hubble space telescope. Many theoretical and experimental works have been devoted to the line shape investigations (Griem, 1964, 1974, 1997; Lesage and Fuhr, 1999; Konjević et al., 2002; NIST, 2003 and references therein). Among them a significant number is dedicated to the neutral helium (He I) spectral lines. Namely, after hydrogen, helium is the most abundant element in the universe. Helium atoms and ions are present in many kinds of cosmic light sources and their radiation is very useful for plasma diagnostical and modeling purposes. In spite of this special role have the 388.86 nm ( $2s \ ^3S_1 - 3p \ ^3P_{2,1,0}^0$  transition), 447.15 nm ( $2p \ ^3P_{2,1}^0 - 4d$

$^3D_{3,2,1}$  transition), 471.32 nm ( $2p\ ^3P_{2,1}^0 - 4s\ ^3S_1$  transition), 501.56 nm ( $2s\ ^1S_0 - 3p\ ^1P_1^0$  transition), 587.56 nm ( $2p\ ^3P_{2,1}^0 - 3d\ ^3D_{3,2,1}$  transition), 667.82 nm ( $2p\ ^1P_1^0 - 3d\ ^1D_2$  transition) and 706.52 nm He I ( $2p\ ^3P_{2,1}^0 - 3s\ ^3S_1$  transition) neutral helium (He I) spectral lines. Recently, these lines have been used in various investigations of the radiation emitted by cosmic light sources like: white dwarfs, variables, supergiants and galaxies (Rupke et al., 2002; Bergeron and Liebert, 2002; Peimbert et al., 2002; Thuan et al., 2002; Bresolin et al., 2002; Benjamin et al., 2002; Drissen et al., 2001; Cuesta and Phillips, 2000). Also, Benjamin et al. (2002) have used some of these lines to investigate the radiative transfer effects for a spherically symmetric nebula with no systematic velocity gradients. Izotov et al. (2001) used some of these lines to derive the  $^4\text{He}$  abundance in the Metal-deficient Blue Compact Dwarf Galaxies Tol 1214-277 and Tol 65<sup>1</sup>, too. Special role has the 667.82 nm line, which is in the work by Harvin et al. (2002) used to investigate the physical properties of the Massive Compact Binary in the Triple Star System HD 36486 ( $\delta$  Orionis A). The 587.56 nm spectral line has been used by Labrosse and Gouttebroze (2001) to estimate the formation of the helium spectrum in solar quiescent prominences and, also, by Muglach and Schmidt (2001) to determine the height and dynamics of the quiet solar chromosphere at the limb. The 706.52 nm line was used for various astrophysical investigations (see Branch et al., 2002; Fransson et al., 2002; Vázquez et al., 2002; Webb et al., 2002). Therefore, the use of these He I spectral lines for diagnostic purposes in astrophysics implies the knowledge of their line profile characteristics.

In plasmas with electron densities ( $N$ ) higher than  $10^{21}\text{ m}^{-3}$ , where the Stark effect begins to play an important role by the He I spectral lines broadening, the knowledge of the Stark broadening characteristics is necessary. A significant number of theoretical and experimental studies are devoted to the He I Stark FWHM (full-width at half intensity maximum,  $W$ ) investigations (Lesage and Fuhr, 1999 and references therein). The aim of this work is to present measured Stark broadening parameters of the mentioned He I spectral lines at (8000 - 33000) K electron temperatures ( $T$ ) and at electron densities of  $(0.3 - 8.2)\times 10^{22}\text{ m}^{-3}$ . The  $T$ -values used are typical of many cosmic light sources. Using a deconvolution procedure, described in Milosavljević and Poparić (2001) and already applied in the case of some He I, Ne I, Ar I and Kr I lines (Milosavljević and Djeniže, 2002abc, 2003ab), on the basis of the observed line profile asymmetry, the characteristics of the ion contribution to the total Stark FWHM ( $W_t$ ) expressed in term of the ion contribution parameter ( $A$ ) and ion-dynamic effect ( $D$ ) (Griem, 1974; Bassalo et al., 1982; Barnard et al., 1974) have been obtained. The separate electron ( $W_e$ ) and ion ( $W_i$ ) contributions to the total Stark width ( $W_t$ ) of the He I spectral line have also been obtained. As an optically thin plasma source we have used the linear, low-pressure, pulsed arc operated in five various discharge conditions. The  $W_t$ ,  $W_e$ ,  $W_i$  and  $A$  values have been compared to all available theoretical and experimental Stark broadening parameters.

On the basis of the precisely recorded He I line shapes, the basic plasma parameters i.e. electron temperature ( $T^D$ ) and electron density ( $N^D$ ) have also been obtained. To the knowledge of this author, the results of the  $T$  and  $N$  values are the first published data obtained directly from the line deconvolution procedure. Plasma parameters have been also measured ( $T^{exp}$  and  $N^{exp}$ ) using independent, well-known, experimental diagnostic techniques. Excellent agreement was found among the two sets of the obtained parameters ( $T^D$  and  $T^{exp}$ ; and  $N^D$  and  $N^{exp}$ ) making it justified to

recommend our deconvolution procedure for plasma diagnostical purposes, especially in astrophysics where direct measurements of the plasma parameters (T and N) are not possible.

## 2. THEORETICAL BACKGROUND

The total line Stark FWHM ( $W_t$ ) is given as

$$W_t = W_e + W_i, \quad (1)$$

where  $W_e$  and  $W_i$  are the electron and ion contributions, respectively. For a non-hydrogenic, isolated neutral atom line the ion broadening is not negligible and the line profiles are described by an asymmetric K function (see Eq. (6) in Chapter 3 and in Milosavljević and Poparić, 2001). The total Stark width ( $W_t$ ) may be calculated (Griem, 1974; Kelleher, 1981; Barnard et al., 1974) from the equation:

$$W_t \approx W_e[1 + 1.75AD(1 - 0.75R)], \quad (2)$$

$$\text{where} \quad R = \sqrt[6]{\frac{36 \cdot \pi \cdot e^6 \cdot N}{(kT)^3}}, \quad (3)$$

is the ratio of the mean ion separation to the Debye length. N and T represent electron density and temperature, respectively. A is the quasi-static ion broadening parameter (see Eq. (224) in Griem, 1974) and D is a coefficient of the ion-dynamic contribution with the established criterion:

$$D = \frac{1.36}{1.75 \cdot (1 - 0.75 \cdot R)} \cdot B^{-1/3} \quad \text{for} \quad B < \left(\frac{1.36}{1.75 \cdot (1 - 0.75 \cdot R)}\right)^3;$$

$$\text{or} \quad D = 1 \quad \text{for} \quad B \geq \left(\frac{1.36}{1.75 \cdot (1 - 0.75 \cdot R)}\right)^3, \quad (4)$$

$$\text{where} \quad B = A^{1/3} \cdot \frac{4.03 \cdot 10^{-7} \cdot W_e[nm]}{(\lambda[nm])^2} \cdot (N[m^{-3}])^{2/3} \cdot \sqrt{\frac{\mu}{T_g[K]}} < 1; \quad (5)$$

is the factor with atom-ion perturber reduced mass  $\mu$  (in amu) and gas temperature  $T_g$ . When  $D = 1$  the influence of the ion-dynamic is negligible and the line shape is treated using the quasi-static ion approximation. From Eqs. (1-6) it is possible to obtain the plasma parameters (N and T) and the line broadening characteristics ( $W_t$ ,  $W_e$ ,  $W_i$ , A and D). One can see that the ion contribution, expressed in terms of the A and D parameters directly determines the ion width ( $W_i$ ) component in the total Stark width (Eqs. (1) and (2)).

### 3. NUMERICAL PROCEDURE FOR DECONVOLUTION

The proposed functions for various line shapes, Eq. (6) are of the integral form and include several parameters. Some of these parameters can be determined in separate experiments, but not all of them. Furthermore, it is impossible to find an analytical solution for the integrals and methods of numerical integration have to be applied. This procedure, combined with the simultaneous fitting of several free parameters, causes the deconvolution to be an extremely difficult task and requires a number of computer supported mathematical techniques. Particular problems are the questions of convergence and reliability of the deconvolution procedure, which are tightly connected with the quality of experimental data.

$$K(\lambda) = K_o + K_{\max} \int_{-\infty}^{\infty} \exp(-t^2) \cdot \left[ \int_0^{\infty} \frac{H_R(\beta)}{1 + \left(2 \frac{\lambda - \lambda_o - \frac{W_G}{2\sqrt{\ln 2}} \cdot t}{W_e} - \alpha \cdot \beta^2\right)^2} \cdot d\beta \right] \cdot dt. \quad (6)$$

Here  $K_o$  is the baseline (offset) and  $K_{\max}$  is the maximum of intensity (intensity for  $\lambda = \lambda_o$ ) (Milosavljević and Poparić, 2001).  $H_R(\beta)$  is an electric microfield strength distribution function of normalized field strength  $\beta = F/F_o$ , where  $F_o$  is the Holtsmark field strength.  $A$  ( $\alpha = A^{4/3}$ ) is the static ion broadening parameter and is a measure of the relative importance of ion and electron broadenings.  $R$  is the ratio of the mean distance between the ions to the Debye radius (see Eq. 3), i.e. the Debye shielding parameter and  $W_e$  is the electron width (FWHM) in the  $j_{A,R}$  profile (Griem, 1974).

For the purpose of deconvolution iteration process we need to know the value of  $K$  (Eq. (6)) as a function of  $\lambda$  for every group of parameters ( $K_{\max}$ ,  $\lambda_o$ ,  $W_e$ ,  $W_G$ ,  $R$ ,  $A$ ).  $W_G$  is defined in Eq.(2.3) in Milosavljević and Poparić (2001). The used numerical procedure for the solution of Eq. (6) is described in earlier publications Milosavljević and Poparić (2001), Milosavljević (2001) and Milosavljević et al. (2002abc). It should be noted that the application of a deconvolution and fitting method requires some assumptions or prior knowledge about plasma condition. Accordingly, for each emitter ionization stage one needs to know the electric microfield distribution, in order to fit the  $K$  functions. In the cases of quasi-static or quasi-static and dynamic broadening, our fitting procedure gives the electron impact width ( $W_e$ ), static ion broadening parameter ( $A$ ) and, finally dynamic ion broadening parameter ( $D$ ).

### 4. EXPERIMENT

The modified version of the linear low-pressure pulsed arc (Milosavljević et al., 2002abc; Milosavljević, 2001; Milosavljević et al., 2000, 2001; Djenize et al., 1998, 2001, 2002ab) has been used as a plasma source. A pulsed discharge was driven in a pyrex discharge tube at different inner diameters and plasma lengths. Various dimensions of the discharge tube offer the possibility of the electron temperature variation in a wide range. The working gas was helium - nitrogen - oxygen mixture (90% He + 8% N<sub>2</sub> + 2% O<sub>2</sub>). The used tube geometry and corresponding discharge conditions are presented in Table. 1.

Table 1: Various discharge conditions. C-bank capacity (in  $\mu\text{F}$ ), U-bank voltage (in kV), H-plasma length (in cm),  $\Phi$ -tube diameter (in mm), P-filling pressure (in Pa).  $N^{\text{exp}}$  (in  $10^{22}\text{m}^{-3}$ ) and  $T^{\text{exp}}$  (in  $10^3\text{K}$ ) denotes measured electron density and temperature, respectively, obtained at a  $25^{\text{th}}$   $\mu\text{s}$  for index 1 and at a  $120^{\text{th}}$   $\mu\text{s}$  for index 2 after the beginning of the discharge when the line profiles were analyzed.  $N_1^{\text{D}}$  (in  $10^{22}\text{m}^{-3}$ ) and  $T_1^{\text{D}}$  (in  $10^3\text{K}$ ) are values obtained using line deconvolution procedure at a  $25^{\text{th}}$   $\mu\text{s}$ .

Exp.	C	U	H	$\Phi$	P	$N_1^{\text{exp}}$	$N_1^{\text{D}}$	$N_2^{\text{exp}}$	$T_1^{\text{exp}}$	$T_1^{\text{D}}$	$T_2^{\text{exp}}$
a	8	4.5	6.2	5	267	6.1	5.4	0.7	33.0	31.4	16.0
b <sub>1</sub>	14	4.2	14.0	25	267	8.2	7.5	0.9	31.5	30.5	14.5
b <sub>2</sub>	14	3.4	14.0	25	267	6.7	6.9	0.8	30.0	30.2	14.0
b <sub>3</sub>	14	2.6	14.0	25	267	4.4	4.0	0.3	28.0	27.1	12.5
b <sub>4</sub>	14	1.5	7.2	5	133	5.0	4.9	0.6	18.0	17.6	8.0

Spectroscopic observation of spectral lines was made end-on along the axis of the discharge tube.

The line profiles were recorded by a step-by-step technique using a photomultiplier (EMI 9789 QB and EMI 9659B) and a grating spectrograph (Zeiss PGS-2, reciprocal linear dispersion 0.73 nm/mm in the first order) system. The instrumental FWHM of 8 pm was obtained by using narrow spectral lines emitted by the hollow cathode discharge. The spectrograph exit slit (10  $\mu\text{m}$ ) with the calibrated photomultipliers was micrometrically traversed along the spectral plane in small wavelength steps (7.3 pm). The averaged photomultiplier signal (five shots in each position) was digitized using an oscilloscope, interfaced to a computer. A sample output, is shown in Figs. 1 and 2.

Plasma reproducibility was monitored by the He I (501.5 nm, 388.8 nm and 587.6 nm) lines radiation and, also, by the discharge current using Rogowski coil signal (it was found to be within  $\pm 5\%$ ).

The used deconvolution procedure in its details is described in Milosavljević and Poparić (2001) and Milosavljević (2001) and, briefly in Chapter 3. The measured profiles were convoluted due to the convolutions of the Lorentzian Stark and Gaussian profiles caused by Doppler and instrumental broadenings (Griem, 1974). Van der Waals and resonance broadenings (Griem, 1974) were estimated to be smaller by more than an order of magnitude in comparison to Stark, Doppler and instrumental broadenings. The deconvolution procedure was computed using the least Chi-square function (see Chapter 3).

The plasma parameters were determined using standard diagnostics methods. Thus, the electron temperature was determined from the ratios of the relative line intensities of four N III spectral lines (409.74 nm, 410.34 nm, 463.42 nm and 464.06 nm) to the 463.05 nm N II spectral line with an estimated error of  $\pm 10\%$ , assuming the existence of the LTE (Griem, 1974). All the necessary atomic data have been taken from NIST (2003) and Glenzer et al. (1994). The electron density decay was measured using a well-known single wavelength He-Ne laser interferometer technique for the 632.8 nm transition with an estimated error of  $\pm 9\%$ . The experimental elec-

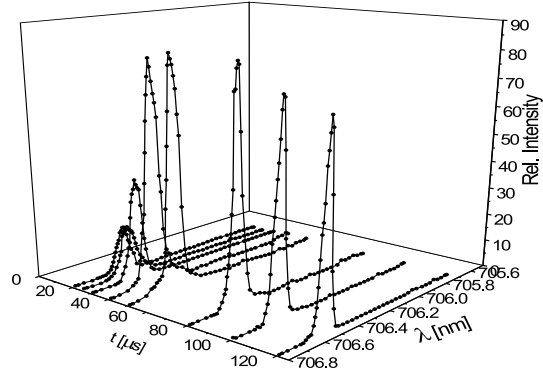


Fig. 1: Temporal evolution of the 706.52 nm He I line profile recorded under discharge conditions  $C=14\mu\text{F}$  and  $U=1.5\text{ kV}$  (see Table 1).

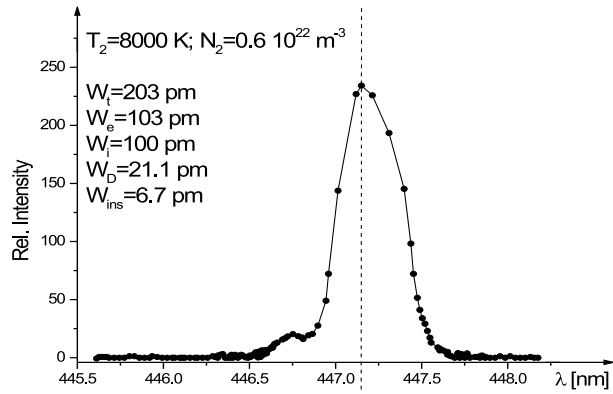


Fig. 2: Recorded profile of the 447.15 nm line at a given  $T$  and  $N$ .  $W_t$ ,  $W_e$ ,  $W_i$ ,  $W_D$ ,  $W_{\text{ins}}$ , represents total, electron and ion Stark width, Doppler and instrumental width, respectively.

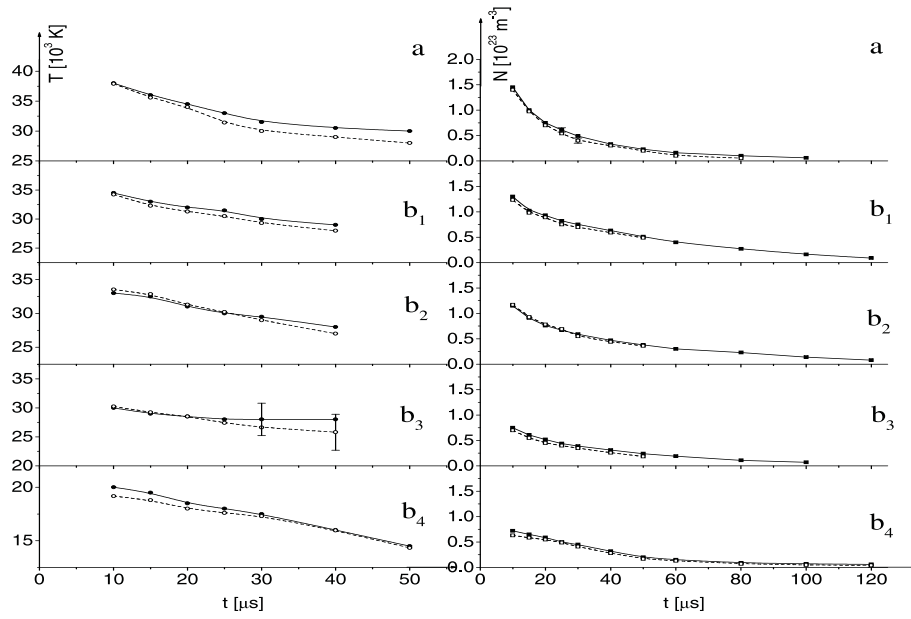


Fig. 3: Electron temperature ( $T$ ) and density ( $N$ ) decays. Full lines represent measured data using independent experimental techniques. Dashed lines represent plasma parameters obtained using our line deconvolution procedure in various plasmas (see Table 1). Error bars, indicated only in the case of the greatest disagreement ( $T$  in  $b_3$ ), represent estimated accuracies of the measurements ( $\pm 10\%$ ) and deconvolutions ( $\pm 12\%$ ).

tron densities ( $N^{exp}$ ) and temperatures ( $T^{exp}$ ), obtained at the moment when the line profiles were analyzed, are presented in Table 1 together with the  $N^D$  and  $T^D$  values obtained from deconvolution procedures.

## 5. RESULTS AND DISCUSSION

The measured  $N^{exp}$  and  $T^{exp}$  decays are presented in Fig. 3 together with the  $N^D$  and  $T^D$  values obtained using the line profile deconvolution procedure, as an example for the 706.52 nm He I line. One can conclude that the agreement among  $N^{exp}$  and  $N^D$  values is excellent (within 4% on the average in the investigated five plasmas). This fact confirms the homogeneity of plasmas in the linear part of our light source (Fig. 1 in Djenize et al., 1998). In the case of the electron temperature the situation is similar but the agreement among the two sets of the electron temperature decays is poorer. This can be explained taking into account the nature of the applied method of the measurement of the electron temperature. Namely, it should be remarked that the uncertainty of the used experimental method (Saha equation) depends on the existence of the LTE during the plasma decay. Existence of the LTE is estimated in the phases of the plasma decay when the electron concentration fulfills the criterion of the existence of the LTE (Griem, 1974, 1997). In our experiment N II and N III energy level (used in the Saha equation) populations remain in the LTE up to 50  $\mu$ s after the beginning of the discharge (in all experiments). After this moment the Saha equation gives unreliable results. Within the experimental accuracy ( $\pm 10\%$ ) of the electron temperature measurements and the uncertainties ( $\pm 12\%$ ) of the  $T^D$  values obtained using the line deconvolution procedure, the  $T^{exp}$  and  $T^D$  values mutually agree up to 50  $\mu$ s after the beginning of the discharge confirming our estimations about the existence of the LTE. This statement also confirms the homogeneity of the created plasmas.

The plasma broadening parameters ( $W_t$ ,  $W_e$ ,  $W_i$ ,  $A$ ,  $D$ ) obtained by our deconvolution procedure of the recorded line profiles at a measured  $N$  and  $T$  values are presented in Tables 2 and 3 together with other authors' results. Various theoretical (G, BCW, DSB) predictions of the  $W_e$ ,  $W_i$ , and  $A$  are also given. By the normalization of the  $A^G$  and  $A^{BCW}$  values to our electron density the well known  $N^{1/4}$  numerical factor (Griem, 1974) was used.

In order to make the comparison among measured ( $W_t^{exp}$ ) and calculated ( $W_t^{th}$ ) total (electron + ion) width values easier, the  $W_t^{exp}/W_t^{th}$  dependence on the electron temperature is presented graphically in Figs. 4 - 10 for the investigated lines.

The  $W_t^G$  (Griem, 1974) and  $W_t^{BCW}$  (Bassalo et al., 1982) values are calculated using Eq. (226) from Griem (1974) with the  $W_e$  and  $A$  values predicted by the G (Griem, 1974) and BCW (Bassalo et al., 1982) theoretical approaches, respectively. The  $W_t^{exp}/W_t^{th}$  ratios related to the Dimitrijević and Sahal – Bréchet (1990) data have been calculated only for our experimental values. Namely, for the  $W_t^{DSB}$  calculations it is necessary to know the helium ion concentration connected to the plasma composition. We have performed this for our discharge conditions only.

It turns out that our  $W_e^{exp}$  and  $W_i^{exp}$  are the first separated experimental electron and ion Stark width data obtained by using the deconvolution procedure (Milosavljević and Poparić, 2001). The broadening parameter ( $W_t^{exp}$ ) represents the first measured value at electron densities higher than  $10^{22}$  m $^{-3}$ .  $W_e^{exp}$  data are smaller than the G, BCW and DSB approximations yield for the three investigated lines (388.86,

Table 2: Line Broadening characteristics. Measured: total Stark FWHM ( $W_t^{exp}$  in pm within  $\pm 12\%$  accuracy), electron and ion ( $\text{He}^+$ ) Stark widths ( $W_e^{exp}$  and  $W_i^{exp}$  in pm within  $\pm 12\%$  accuracy), quasistatic ion broadening parameter ( $A^{exp}$ , dimensionless within  $\pm 15\%$  accuracy) and ion dynamic coefficient ( $D^{exp}$ , dimensionless within  $\pm 20\%$  accuracy) at measured electron temperatures ( $T^{exp}$  in  $10^3$  K) and electron densities ( $N^{exp}$  in  $10^{22}\text{m}^{-3}$ ). Ref presents: Tw, this work; RS, Roder and Stampa (1964); K, Kelleher (1981); SK, Solwitsch and Kusch (1979); B, Berg et al. (1962); W, Wulff (1958); Ku, Kusch (1971); KK, Kobilarov et al. (1989); Gr, Griem et al. (1962); ES, Einfeld and Sauerbrey (1976); C, Chaing et al. (1977); L, Lincke (1964); GJ, Greig and Jones (1970); BR, Böttcher et al. (1963); P, Pérez et al. (1991); M, Mijatović et al. (1995); MS, Mazing and Slemzin (1973); PL, Purić et al. (1970); BG, Büscher et al. (1995); Ga, Gauthier et al. (1981); VK, Vujičić and Kobilarov (1988). The indexes G, BCW and DSB denote theoretical data taken from Griem (1974), Bassalo et al. (1982) and Dimitrijević and Sahal – Bréchet (1990), respectively at a given T and N. The wavelengths (i.e. 5876, 6678 and 4472) are given in  $10^{-10}$  m.

$T^{exp}$	$N^{exp}$	$W_t^{exp}$	$W_e^{exp}$	$W_i^{exp}$	$A^{exp}$	$D^{exp}$	Ref.	$W_e^G$	$W_e^{BCW}$	$W_e^{DSB}$	$W_i^{DSB}$	$A^G$	$A^{BCW}$
							5876						
33.0	6.1	210	172	38	0.163	1.46	Tw	215	156	183	42	0.093	0.118
31.5	8.2	268	218	50	0.176	1.40	Tw	289	213	246	55	0.100	0.127
30.0	6.7	218	179	39	0.167	1.46	Tw	237	175	201	45	0.095	0.120
28.0	4.4	151	126	25	0.150	1.57	Tw	155	117	132	29	0.086	0.108
18.0	5.0	150	126	24	0.156	1.60	Tw	176	134	150	31	0.088	0.108
20.9	1.03	39					K						
45.0	15.9	550					B						
31.0	5.4	200					KK						
16.5	1.7				0.05*		RS						
3.70	2.25	91					PL						
52.0	10.2	3160					BG						
							6678						
33.0	6.1	481	298	183	0.459	1.18	Tw	397	345	358	170	0.282	0.309
31.5	8.2	628	370	258	0.498	1.12	Tw	533	467	502	226	0.300	0.328
30.0	6.7	512	315	197	0.474	1.17	Tw	439	389	402	181	0.282	0.306
28.0	4.4	337	216	121	0.420	1.27	Tw	290	257	266	117	0.252	0.265
18.0	5.0	361	240	121	0.413	1.26	Tw	358	323	323	124	0.249	0.271
20.9	1.03	98					K						
30.1	3.2	231					P						
19.3	0.25	22					M						
20.0	10.0	960					Ga						
26.0	7.1	620					VK						
							4472						
16.0	0.7	237	106	131	0.917	1.0	Tw	162	150	140	113	0.636	0.668
14.5	0.9	316	145	171	0.911	1.0	Tw	212	200	185	142	0.668	0.704
14.0	0.8	258	120	138	0.883	1.0	Tw	190	180	165	125	0.642	0.675
12.5	0.3	101	48	53	0.806	1.03	Tw	73	69	63	45	0.491	0.517
8.0	0.6	203	103	100	0.825	1.0	Tw	155	147	134	82	0.554	0.574
20.9	1.03	109					K						
20.0	13	4500					B						

Table 3: Same as in Table 2. The wavelengths (i.e. 3889, 5016, 7065 and 4713) are given in  $10^{-10}$  m.

$T^{exp}$	$N^{exp}$	$W_t^{exp}$	$W_e^{exp}$	$W_i^{exp}$	$A^{exp}$	$D^{exp}$	Ref.	$W_e^G$	$W_e^{BCW}$	$W_e^{DSB}$	$W_i^{DSB}$	$A^G$	$A^{BCW}$
							3889						
33.0	6.1	139	110	29	0.196	1.26	Tw	143	120	116	28	0.105	0.119
31.5	8.2	185	145	40	0.212	1.19	Tw	192	162	155	37	0.113	0.128
30.0	6.7	149	118	31	0.202	1.25	Tw	157	132	126	30	0.108	0.122
28.0	4.4	96	78	18	0.181	1.37	Tw	103	87	82	15	0.097	0.110
18.0	5.0	103	83	20	0.190	1.37	Tw	116	97	90	21	0.101	0.114
15.0	0.72				0.04*		RS						
20.9	1.03	24					K						
20.0	6.7	170					SK						
26.0	15.0	450					B						
30.0	3.2	73					W						
18.0	0.8	33					Ku						
36.0	6.1	151					KK						
30.0	2.7	74					Gr						
							5016						
33.0	6.1	452	279	173	0.460	1.0	Tw	384	354	336	134	0.277	0.293
31.5	8.2	602	365	237	0.496	1.0	Tw	518	481	453	179	0.295	0.314
30.0	6.7	481	294	187	0.486	1.0	Tw	427	395	372	145	0.279	0.296
28.0	4.4	312	198	114	0.433	1.08	Tw	282	262	246	95	0.249	0.265
18.0	5.0	332	218	114	0.427	1.07	Tw	340	315	289	100	0.252	0.263
14.1	0.38				0.14*		RS						
20.9	1.03	85					K						
20.0	6.7	54					SK						
24.0	16.5	1300					B						
30.0	3.2	190					W						
26.0	4.6	75					Ku						
30.0	2.3	182					Gr						
38.0	3.6	290					ES						
17.4	10.5	960					C						
22.7	9.3	720					L						
25.0	2.7	277					GJ						
16.9	2.0	160					BR						
30.15	3.23	237					P						
23.6	0.59	47					M						
							7065						
33.0	6.1	281	234	47	0.148	1.51	Tw	307	273	224	46	0.082	0.089
31.5	8.2	372	307	65	0.160	1.42	Tw	411	361	298	58	0.089	0.099
30.0	6.7	300	250	50	0.152	1.49	Tw	333	292	241	51	0.085	0.094
28.0	4.4	190	161	29	0.136	1.65	Tw	217	190	156	29	0.077	0.085
18.0	5.0	211	179	32	0.145	1.62	Tw	232	203	171	26	0.083	0.092
20.9	1.03	47			0.031*	2.33*	K						
21.4	0.34	17					M						
22.7	0.45	22					M						
23.6	0.59	29					M						
34.8	1.0	51					MS						
							4713						
33.0	6.1	542	371	171	0.343	1.0	Tw	554	483	398	95	0.146	0.162
31.5	8.2	713	481	232	0.368	1.0	Tw	740	648	533	125	0.157	0.175
30.0	6.7	595	407	188	0.352	1.0	Tw	603	528	430	99	0.150	0.166
28.0	4.4	372	261	111	0.317	1.0	Tw	394	341	281	65	0.136	0.151
18.0	5.0	403	286	117	0.335	1.0	Tw	428	370	319	69	0.142	0.161
16.5	1.7				0.20*		RS						
20.9	1.03	96					K						
20.0	13.0	1400					B						
30.0	2.6	300					Gr						
22.7	9.3	91					L						
30.2	3.23	295					P						
19.3	0.25	23					M						

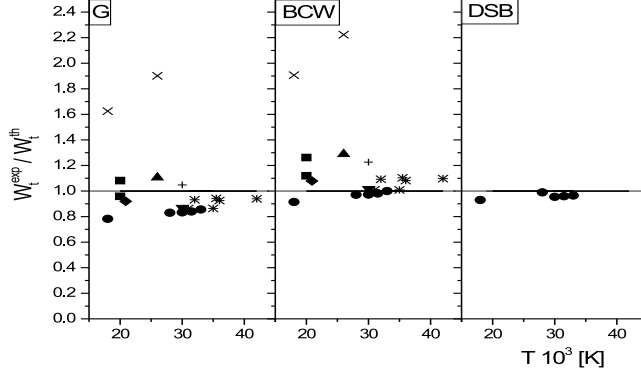


Fig. 4: Ratios of the experimental total Stark FWHM ( $W_t^{exp}$ ) to the various theoretical ( $W_t^{th}$ ) predictions vs. electron temperature for the He I 388.86 nm line.  $\bullet$ ,  $+$ ,  $\blacklozenge$ ,  $\blacksquare$ ,  $\blacktriangle$ ,  $\blacktriangledown$ ,  $\times$  and  $*$  represent our experimental data and those from Griem et al. (1962), Kelleher (1981), Solwitsch and Kusch (1979), Berg et al. (1962), Wulff (1958), Kusch (1971) and Kobilarov et al. (1989), respectively. G, BCW and DSB represent the ratios related to the theories taken from Griem (1974), Bassalo et al. (1982) and Dimitrijević and Sahal – Bréchet (1990), respectively.

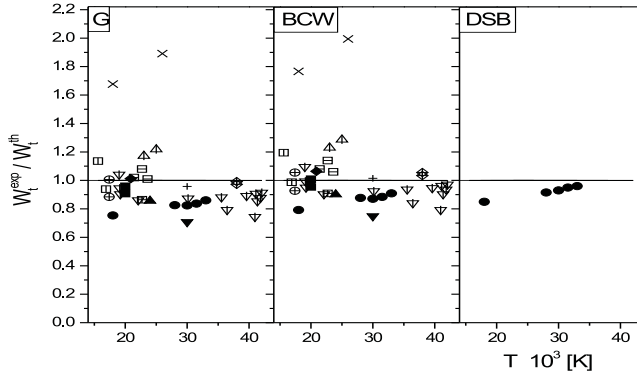


Fig. 5: Ratios of the experimental total Stark FWHM ( $W_t^{exp}$ ) to the various theoretical ( $W_t^{th}$ ) predictions vs. electron temperature for the 501.56 nm He I line.  $\bullet$ ,  $+$ ,  $\blacklozenge$ ,  $\blacksquare$ ,  $\blacktriangle$ ,  $\blacktriangledown$ ,  $\times$ ,  $\blacklozenge$ ,  $\oplus$ ,  $\boxplus$ ,  $\blacktriangle$ ,  $\blacktriangledown$  and  $\boxminus$  represent our experimental data and those from Griem et al. (1962), Kelleher (1981), Solwitsch and Kusch (1979), Berg et al. (1962), Wulff (1958), Kusch (1971), Einfeld and Sauerbrey (1976), Chaing et al. (1977), Lincke (1964), Greig and Jones (1970), Bötticher et al. (1963), Pérez et al. (1991) and Mijatović et al. (1995), respectively. G, BCW and DSB represent the ratios related to the theories taken from Griem (1974), Bassalo et al. (1982) and Dimitrijević and Sahal – Bréchet (1990), respectively.

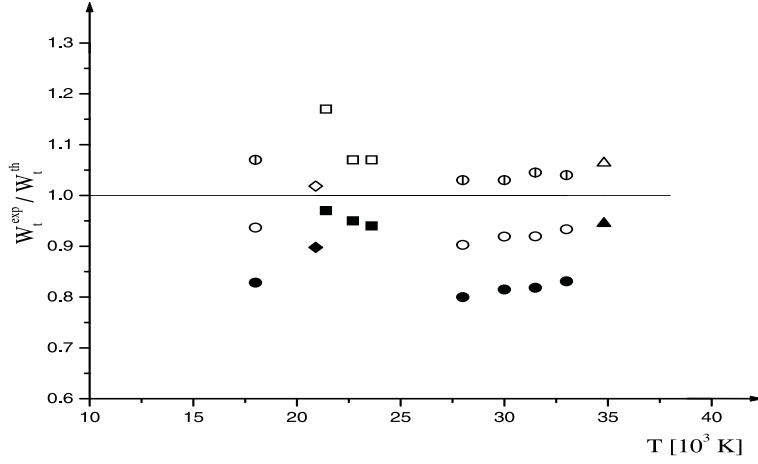


Fig. 6: Ratios of the experimental total Stark FWHM ( $W_t^{\text{exp}}$ ) to the various theoretical ( $W_t^{\text{th}}$ ) predictions vs. electron temperature for the He I 706.52 nm line. Circle, diamond, triangle and square represent our experimental data and those from Kelleher (1981), Mazing and Slemzin (1973) and Mijatović et al. (1995), respectively. Filled, empty and half divided symbols represent the ratios related to the theories taken from Griem (1974), Bassalo et al. (1982) and Dimitrijević and Sahal – Bréchet (1990), respectively.

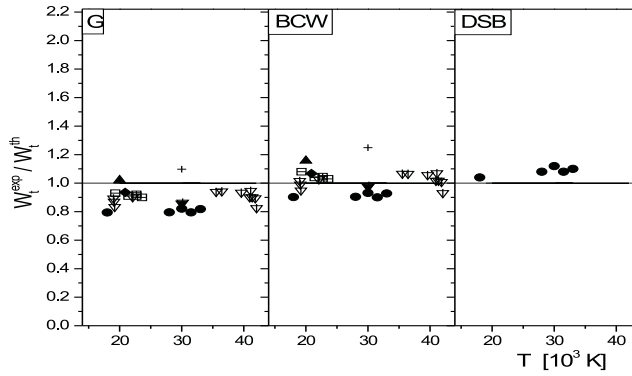


Fig. 7: Ratios of the experimental total Stark FWHM ( $W_t^{\text{exp}}$ ) to the various theoretical ( $W_t^{\text{th}}$ ) predictions vs. electron temperature for the He I 471.32 nm line.  $\bullet$ ,  $+$ ,  $\blacklozenge$ ,  $\blacktriangle$ ,  $\blacktriangledown$ ,  $\boxplus$ ,  $\blacktriangledown$  and  $\boxminus$  represent our experimental data and those from Griem et al. (1962), Kelleher (1981), Berg et al. (1962), Wulff (1958), Lincke (1964), Pérez et al. (1991) and Mijatović et al. (1995), respectively. G, BCW and DSB represent the ratios related to the theories taken from Griem (1974), Bassalo et al. (1982) and Dimitrijević and Sahal – Bréchet (1990), respectively.

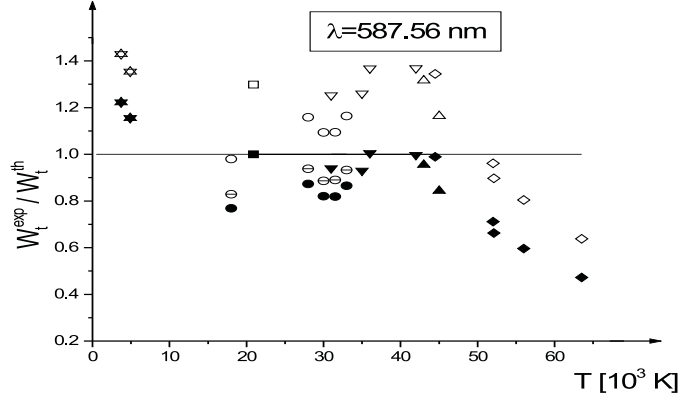


Fig. 8: Ratios of the experimental total Stark FWHM ( $W_t^{\text{exp}}$ ) to the various theoretical ( $W_t^{\text{th}}$ ) predictions vs. electron temperature for the He I  $\lambda=587.56$  nm.  $\circ$ ,  $\diamond$ ,  $\nabla$ ,  $\triangle$ ,  $\square$  and  $\star$  represent our experimental data and those from Büscher et al. (1995), Kobilarov et al. (1989), Berg et al. (1962), Kelleher (1981), and Purić et al. (1970), respectively. Filled, empty and half divided symbols represent the ratios related to the theories taken from Griem (1974), Bassalo et al. (1982) and Dimitrijević and Sahal – Bréchet (1990), respectively.

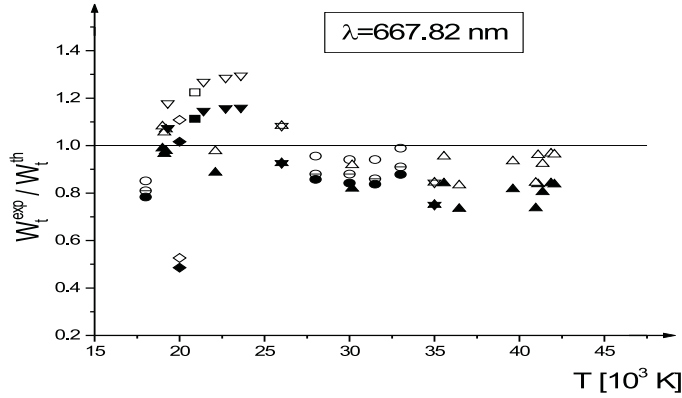


Fig. 9: Ratios of the experimental total Stark FWHM ( $W_t^{\text{exp}}$ ) to the various theoretical ( $W_t^{\text{th}}$ ) predictions vs. electron temperature for the He I  $\lambda=667.82$  nm.  $\circ$ ,  $\diamond$ ,  $\nabla$ ,  $\triangle$ ,  $\square$  and  $\star$  represent our experimental data and those from Gauthier et al. (1981), Mijatović et al. (1995), Pérez et al. (1991), Kelleher (1981), and Vujičić and Kobilarov (1988), respectively. Filled, empty and half divided symbols represent the ratios related to the theories taken from Griem (1974), Bassalo et al. (1982) and Dimitrijević and Sahal – Bréchet (1990), respectively.

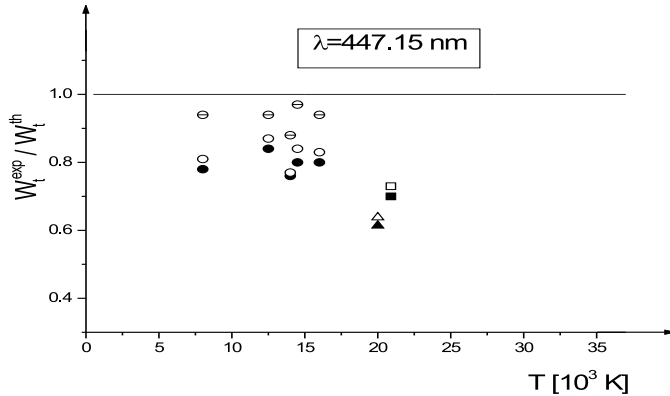


Fig. 10: Ratios of the experimental total Stark FWHM ( $W_t^{\text{exp}}$ ) to the various theoretical ( $W_t^{\text{th}}$ ) predictions vs. electron temperature for the He I  $\lambda = 447.15$  nm.  $\circ$ ,  $\triangle$  and  $\square$  represent our experimental data and those from Berg et al. (1962) and Kelleher (1981), respectively. Filled, empty and half divided symbols represent the ratios related to the theories taken from Griem (1974), Bassalo et al. (1982) and Dimitrijević and Sahal – Bréchet (1990), respectively.

501.56 and 471.32 nm). The highest disagreement was found with the 501.56 nm line. In this case  $W_e^{\text{exp}}$  lie 27% below  $W_e^G$  and about 20% below  $W_e^{\text{BCW}}$  and  $W_e^{\text{DSB}}$  values. Approximations BCW and DSB yield smaller  $W_e$  values than the G approximation. In the case of the 388.86 nm line the  $W_e^{\text{exp}}$  and  $W_e^{\text{DSB}}$  values show a tolerable mutual agreement (within  $\pm 16\%$ ). They are in excellent agreement (within  $\pm 4\%$ ) with  $W_e^{\text{DSB}}$  and (within  $\pm 8\%$ ) with  $W_i^{\text{DSB}}$  (Dimitrijević and Sahal – Bréchet, 1990) values for the 706.52 nm spectral line. Theoretical  $W_e^G$  (Griem, 1974) and  $W_e^{\text{BCW}}$  (Bassalo et al., 1982) values are higher than ours by about 33% and 17% (on the average), respectively, for this line. The  $W_e^{\text{exp}}$  results are smaller than the G approximation for the other three investigated lines (447.15, 587.56 and 667.82 nm). The greatest disagreement was found for the 447.15 nm line. It amounts to about 53%. The other two approximations (BCW and DSB), in the case of the 667.82 nm and 447.15 nm lines, yield smaller  $W_e$  values than the G approximation, but they are also higher than ours. For the 587.56 nm line the  $W_e^{\text{exp}}$ ,  $W_e^{\text{BCW}}$  and  $W_e^{\text{DSB}}$  values show a reasonable mutual agreement (within  $\pm 12\%$  experimental accuracy). This indicated that the  $W_e$  values calculated by Freudenstein and Cooper (1978) and Dimitrijević and Konjević (1986), for the 667.82 nm line, exceed all other  $W_e$  data presented in Table 2.

By the inspection of Figs. 4–10 one can conclude that Griem’s (1974)  $W_t$  values lie above most of the experimental values and also above BCW and DSB theoretical data. This is well evident in the case of the 471.32 nm line (see Fig. 7). Theoretical  $W_t$  values presented by Bassalo et al. (1982) lie about 10% - 15% below Griem’s values. The  $W_t$  values ( $W_e + W_i$ ) presented by Dimitrijević and Sahal – Bréchet (1990) agree with the ( $W_t^{\text{exp}}$ ) within 3% - 10% (on the average) with the best agreement in the case of the 388.86 nm line (see Fig. 4). It should be pointed out that experimental

$W_t^{exp}$  values are smaller than the G, BCW and DSB theories yield in the case of the 501.56 nm spectral line at electron temperatures higher than 25000 K (see Fig. 5). Experimental total half-widths of the 706.52 nm, including ours, agree well (within  $\pm 10\%$ ) with calculated values from Bassalo et al. (1982). Our  $W_t^{exp}$  agree excellently with  $W_t^{DSB}$  from Dimitrijević and Sahal – Bréchet (1990) (see Figure 6). It turns out that our  $W_i^{exp}/W_t^{exp}$  (16% on the average) agree excellently with  $W_i^{DSB}/W_t^{DSB}$  (also 16% on the average) theoretical values (Dimitrijević and Sahal – Bréchet, 1990) for the 706.52 nm spectral line. This is clear in the case of the 667.82 nm line at higher electron temperatures (see Fig. 9). Theoretical  $W_t$  values presented by Bassalo et al. (1982) lie about 10% - 30% below Griem's values. The  $W_t$  values ( $W_e + W_i$ ) presented by Dimitrijević and Sahal – Bréchet (1990) agree with ours ( $W_t^{exp}$ ) to within 3% – 18% with the best agreement for the 447.15 nm line (see Fig. 10).

This constitutes evident contribution of the ion influence to the line broadening due to the quasi-static ion and ion-dynamic effects. The  $A^{exp}$  values are the first data obtained directly by the use of the line deconvolution procedure. They are higher than the G and BCW approaches provide at about: 87% and 67% (for 388.86 nm line), 135% and 110% (for 471.32 nm line), 70% and 61% (for 501.56 nm line), respectively. It has been found that the ion dynamic effect, expressed due to the  $D$  coefficient is negligible ( $D \simeq 1$ ) by our plasma parameters and plasma composition for the 471.32 nm and 501.56 nm lines. In the case of the 388.86 nm line the ion dynamic effect is relatively small ( $D \simeq 1.3$ ). It should be pointed out that we have found good agreement between our  $W_i^{exp}/W_t^{exp}$  and theoretical  $W_i^{DSB}/W_t^{DSB}$  (Dimitrijević and Sahal – Bréchet, 1990) ratio values only in the case of the 388.86 nm (within 10%, on the average). This agreement is within estimated experimental accuracies ( $\pm 12\%$ ) of the  $W_i^{exp}$  and  $W_t^{exp}$  values. In the case of the 471.32 nm and 501.56 nm lines, we have found  $W_i^{exp}/W_t^{exp}$  values that overvalue  $W_i^{DSB}/W_t^{DSB}$  data by about 65% and 35%, respectively. One can conclude that the ion contribution to the total line width plays a more important role than the G, BCW and DSB approximations provide, especially in the case of the 471.32 nm and 501.56 nm lines. The quasi-static ion effect is higher than the G (Griem, 1974) and BCW (Bassalo et al., 1982) approaches estimate by about 70% and 50%, respectively, for 706.52 nm. Besides, it has also been found that the ion-dynamic effect plays an important role concerning this line. This effect multiplies the quasi-static ion influence about 1.5 times with our plasma parameters and composition and show increasing tendency at lower electron densities confirming the theoretical (Griem, 1974; Barnard et al., 1974) estimations. The  $A$  are higher than what the G and BCW approaches yield by about: 75% and 38% (for the 587.56 nm line), 40% and 34% (for the 667.82 nm line), 31% and 28% (for the 447.15 nm line), respectively. Furthermore, it has been found that the ion dynamic effect multiplies the quasi-static ion contribution by about 1.5 for the 587.56 nm line and 1.2 for the 667.82 nm line. For the 447.15 nm line the ion dynamic effect is negligible ( $D=1$ ). It should be pointed out that we have found good agreement between our  $W_i^{exp}/W_t^{exp}$  and theoretical  $W_i^{DSB}/W_t^{DSB}$  (Dimitrijević and Sahal – Bréchet, 1990) ratio values. These are: 18.5% (18.0%), 37.5% (30.5%) and 53% (44%) for the 587.56 nm, 667.82 nm and 447.15 nm lines, respectively. As can be seen, this agreement is within the estimated experimental accuracies ( $\pm 12\%$ ) of the  $W_i^{exp}$  and  $W_t^{exp}$  values for the 587.56 nm and 667.82 nm and 447.15 nm lines. It may be concluded that the ion contribution to the total line width increases with the upper-level energy of the transition and plays a

more important role than what the G and BCW approximations provide.

It turns out that the  $A^{exp}$  values, obtained by Roder and Stampa (1964) and Kelleher (1981), presented with asterisk in Tables 2 and 3, represent the line asymmetry factors obtained at the line half intensity maximum. These are smaller than our  $A^{exp}$  values.

## 6. CONCLUSION

Using line deconvolution procedure (Milosavljević and Poparić, 2001; Milosavljević, 2001) one obtained, on the basis of the precisely recorded HeI spectral line profiles, their Stark broadening parameters:  $W_t$ ,  $W_e$ ,  $W_i$ ,  $A$  and  $D$  and the main plasma parameters (N and T). One finds that the ion contribution to the line profiles plays much more important role than the semiclassical (Griem, 1974; Bassalo et al., 1982) theoretical approximation does which must be taken into account when using these HeI lines to plasma diagnostical purposes according to the estimations made the semiclassical perturbation formalism (Dimitrijević and Sahal – Bréchet, 1990).

**Acknowledgments.** This work is a part of the project "Determination of the atomic parameters on the basis of the spectral line profiles" supported by the Ministry of Science, Technologies and Development of the Republic of Serbia.

## References

- Barnard, A.J., Cooper, J., Smith, E.W.: 1974, *J. Quant. Spectrosc. Radiat. Transfer*, **14**, 1025.
- Bassalo, J.M., Cattani, M., Walder, V.S.: 1982, *J. Quant. Spectrosc. Radiat. Transfer*, **28**, 75.
- Benjamin, R.A., Skillman, E.D., Smits, D.S.: 2002, *Astrophys. J.*, **569**, 288.
- Berg, H.F., Ali, A.W., Lincke, R., Griem, H.R.: 1962, *Phys. Rev.*, **125**, 199.
- Bergeron, P., Liebert, J.: 2002, *Astrophys. J.*, **566**, 1091.
- Böttcher, W., Roder, O., Wobig, K.H.: 1963, *Z. Phys.*, **175**, 480.
- Branch, D., et al.: 2002, *Astrophys. J.*, **566**, 1005.
- Bresolin, F., Gieren, W., Kudritzki, R.-P., Pietrzyński, G., Przybilla, N.: 2002, *Astrophys. J.*, **567**, 277.
- Büscher, S., Glenzer, S., Wrubel, Th., Kunze, H.-J.: 1995, *J. Quant. Spectrosc. Radiat. Transfer*, **54**, 73.
- Chaing, W.T., Murphy, D.P., Chen, Y.G., Griem, H.R.: 1977, *Z. Naturforsch.*, **32a**, 818.
- Cuesta, L., Phillips, J.P.: 2000, *Astrophys. J.*, **543**, 754.
- Dimitrijević, M.S., Konjević, N.: 1986, *Astron. Astrophys.*, **163**, 297.
- Dimitrijević, M.S., Sahal–Bréchet, S.: 1990, *Astron. Astrophys. Suppl. Ser.*, **82**, 519.
- Djeniže, S., Milosavljević, V., Srećković, A.: 1998, *J. Quant. Spectrosc. Radiat. Transfer*, **59**, 71.
- Djeniže, S., Milosavljević, V., Dimitrijević, M.S.: 2002a, *Astron. Astrophys.*, **382**, 359.
- Djeniže, S., Srećković, A., Bukvić, S.: 2002b, *Eur. Phys. J. D.*, **20**, 11.
- Djeniže, S., Bukvić, S.: 2001, *Astron. Astrophys.*, **365**, 252.
- Drissen, L., et al.: 2001, *Astrophys. J.*, **546**, 484.
- Einfeld, D., Sauerbrey, G.: 1976, *Z. Naturforsch.*, **31a**, 310.
- Fransson, C., et al., : 2002, *Astrophys. J.*, **572**, 350.
- Freudenstein, S.A., Cooper, J.: 1978, *Astrophys. J.*, **224**, 1079.
- Gauthier, J.C., Geindre, J.P., Goldbach, C., Grandjouan, N., Mazure, A., Nollez, G.: 1981, *J. Phys. B*, **14**, 2099.
- Glenzer, S., Kunze, H.J., Musielok, J., Kim, Y.K., Wiese, W.L. : 1994, *Phys. Rev. A*, **49**, 221.

- Greig, J.R., Jones, L.A.: 1970, *Phys. Rev. A*, **1**, 1261.
- Griem, H.R.: 1964, *Plasma Spectroscopy*, McGraw-Hill Book Company, New York.
- Griem, H.R.: 1974, *Spectral Line Broadening by Plasmas*, Acad. Press, New York.
- Griem, H.R.: 1997, *Principles of Plasma Spectroscopy*, Univ. Press, Cambridge.
- Griem, R.H., Baranger, M., Kolb, A.C., Oertel, G.: 1962, *Phys. Rev.*, **125**, 177.
- Harvin, J.A., Gies, D.R., Bagnuolo, W.G.Jr., Penny, L.R., Thaller, M.L.: 2002, *Astrophys. J.*, **565**, 1216.
- Izotov, Y.I., Chaffee, F.H., Green, R.F.: 2001, *Astrophys. J.*, **562**, 727.
- Kelleher, D.E.: 1981, *J. Quant. Spectrosc. Radiat. Transfer*, **25**, 191.
- Kobilarov, R., Konjević, N., Popović, M.V.: 1989, *Phys. Rev. A*, **40**, 3871.
- Konjević, N., Lesage, A., Fuhr, J.R., Wiese, W.L.: 2002, *J. Phys. Chem. Ref. Data*, **31**, 819.
- Kusch, H.J.: 1971, *Z. Naturforsch.*, **26a**, 1970.
- Labrosse, N., Gouttebroze, P.: 2001, *Astron. Astrophys.*, **380**, 323.
- Lesage, A., Fuhr, J.R.: 1999, *Bibliography on Atomic Line Shapes and Shifts (April 1992 through June 1999)*, Observatoire de Paris
- Lincke, R.: 1964, *PhD Thesis*, (unpublished), University of Maryland.
- Mazing, M.A., Slemzin, V.A.: 1973, *Sov. Phys. Lebedev Inst. Rep.*, **4**, 42.
- Mijatović, Z., Konjević, N., Ivković, M., Kobilarov, R.: 1995, *Phys. Rev. E*, **51**, 4891.
- Milosavljević, V.: 2001, *PhD Thesis*, (unpublished), University of Belgrade, Faculty of Physics, Belgrade.
- Milosavljević, V., Dimitrijević, M.S., Djeniže, S.: 2001, *Astrophys. J. Supp.*, **135**, 115.
- Milosavljević, V., Djeniže, S., Dimitrijević, M.S., Popović, L.Č.: 2000, *Phys. Rev. E*, **62**, 4137.
- Milosavljević, V., Djeniže, S.: 2002a, *Astron. Astrophys.*, **393**, 721.
- Milosavljević, V., Djeniže, S.: 2002b, *New Astron.*, **(7/8)**, 543.
- Milosavljević, V., Djeniže, S.: 2002c, *Phys. Lett. A*, **305/1-2**, 70.
- Milosavljević, V., Djeniže, S.: 2003a, *Astron. Astrophys.*, **398**, 1179.
- Milosavljević, V., Djeniže, S.: 2003b, *Eur. Phys. J. D.*, **in press**, .
- Milosavljević, V., Poparić, G.: 2001, *Phys. Rev. E*, **63**, 036404.
- Muglach, K., Schmidt, W.: 2001, *Astron. Astrophys.*, **379**, 592.
- NIST : 2003, *Atomic Spectra Data Base Lines*, <http://physics.nist.gov>
- Peimbert, A., Peimbert, M., Luridiana, V.: 2002, *Astrophys. J.*, **565**, 668.
- Pérez, C., de la Rosa, I., de Frutos, A.M., Mar, S.: 1991, *Phys. Rev. A*, **44**, 6785.
- Purić, J., Labat, J., Ćirković, Lj., Konjević, N.: 1970, *Fizika*, **2**, 67.
- Roder, O., Stampa, A.: 1964, *Z. Physik*, **178**, 348.
- Rupke, D.S., Veilleux, S., Sanders, D.B.: 2002, *Astrophys. J.*, **570**, 588.
- Soltwisch, H., Kusch, H.J.: 1979, *Z. Naturforsch.*, **34a**, 300.
- Thuan, T.X., Lecavelier des Etangs A., Izotov, Y.: 2002, *Astrophys. J.*, **565**, 941.
- Vázquez, R., et al., : 2002, *Astrophys. J.*, **576**, 860.
- Vujičić, B.T., Kobilarov, R.: 1988, *9th Int. Conf. Spect. Line Shapes*, Contributed papers, A18, Nicholos Copernicos University press, Torun Poland.
- Webb, N.A., Naylor, T., Jeffries, R.D.: 2002, *Astrophys. J.*, **568**, L45.
- Wulff, H.: 1958, *Z. Physik*, **150**, 614.